Future Journal of Pharmaceutical Sciences

RESEARCH

Open Access

Comprehensive identification of chemical fingerprint and potential quality markers of leaves and roots of two *Aloe* species via LC–MS/MS and computational analyses in relation to anti-virulence activity

Passent M. Abdel-Baki[1*†], Rana M. Ibrahim[1†], Mai E. Hussein[1*], Mohammed Abu-Elghait[2*], Mona Shaban E. M. Badawy[3], Maha Hanafi[4], Mansour Sobeh[5] and Nariman E. Mahdy[1]

Abstract

Background Over the past centuries, *Aloe* species have been traditionally used in managements of infectious ailments. However, no scientific investigation has been conducted into their mechanistic actions behind their antimicrobial activities. The main purpose of this study is to investigate the anti-virulence activities of *Aloe marlothii* A. Berger (AM) and *Aloe striata* Haw (AS) leaves and roots against *Pseudomonas aeruginosa* based on biofilm, pyocyanin and motility assays. Besides, the metabolic profiling of their different organs was evaluated via HPLC–MS/MS analysis. A molecular docking study of marker compounds into a LasR target was conducted to gain an insight into the bioactive metabolites involved into mechanism of action.

Results *A. marlothii* roots (AMR) and *A. striata* leaves (ASL) displayed significant activity against *P. aeruginosa* at 0.5 MIC via decreasing the biofilm development, pyocyanin production, swarming and swimming motilities. HPLC–MS/MS analysis led to the identification of one hundred metabolites belonging to different chemical classes. Additionally, it revealed the richness of AMR and ASL with anthraquinones and anthrones. Molecular docking of tentatively identified anthraquinones and anthrones was performed, revealing that chrysophanol-8-*O*-glucoside and 6-malonylnataloin revealed superior binding affinities and stabilities within the pocket of LasR system, compared to TP-4.

Conclusions These findings give sound evidence for the use of AMR and ASL as effective anti-virulence agents against *P. aeruginosa*.

Keywords *Aloe marlothii*, *Aloe striata*, HPLC–PDA-MS/MS analysis, Molecular docking, Antibiofilm

†Passent M. Abdel-Baki and Rana M. Ibrahim have contributed equally to this work.

*Correspondence:
Passent M. Abdel-Baki
passent.mohamed@pharma.cu.edu.eg
Mai E. Hussein
mai.husein@pharma.cu.edu.eg
Mohammed Abu-Elghait
Dr_abuelghait@azhar.edu.eg
Full list of author information is available at the end of the article

Springer Open

© The Author(s) 2025. **Open Access** This article is licensed under a Creative Commons Attribution 4.0 International License, which permits use, sharing, adaptation, distribution and reproduction in any medium or format, as long as you give appropriate credit to the original author(s) and the source, provide a link to the Creative Commons licence, and indicate if changes were made. The images or other third party material in this article are included in the article's Creative Commons licence, unless indicated otherwise in a credit line to the material. If material is not included in the article's Creative Commons licence and your intended use is not permitted by statutory regulation or exceeds the permitted use, you will need to obtain permission directly from the copyright holder. To view a copy of this licence, visit http://creativecommons.org/licenses/by/4.0/.

Background

Antibiotic resistance is the bacteria's ability to withstand the inhibitory or destructive activity of an antibiotic to which it was not previously resistant [1]. This issue raises major public health concerns since it has a negative impact on infection treatment. According to a recent World Health Organization (WHO) research, antibiotic resistance contributed to more than 4.95 million deaths per year [2]. In addition, it is regarded as a major economic burden as expected by the World Bank to increase the health care costs US$ 1 trillion by 2050 [2].

Pseudomonas aeruginosa (*P. aeruginosa*), a Gram-negative bacterium, is found mainly in the environment and can survive on various surfaces such as medical devices and household drains. Thus, it causes harmful infections in both immunocompromised and immunocompetent hosts as enteritis, urinary tract infections, hematological problems, osteomyelitis, skin infections, transplant-associated infections, and pneumonia [3, 4].

P. aeruginosa is an adaptive organism as being capable of producing different virulence factors. Biofilm is the most important one of them. Biofilm is groups of cells that release extracellular matrix substances which attach the bacteria to various surfaces and protect them from environmental changes. Biofilm matrix is mainly composed of polysaccharides, extracellular DNA (eDNA), proteins, and lipids. Quorum sensing (QS) is a signal transduction pathway utilized by *P. aeruginosa* to communicate with each other for adaptation to environmental stress. Las, Rhl, PQS, and IQS, the distinct pathways in QS, play key roles in the biofilm development by producing the functional elements including pyoverdine, pyocyanin, rhamnolipid, lectins, and Pel polysaccharides [3, 5]. Pyocyanin exhibits a cytotoxic effect due to its low molecular weight and its zwitterionic properties. Its ability to oxidize and reduce other molecules results in the killing of competing microbes against *P. aeruginosa* by disrupting their cells [3, 5, 6].

As a result, the concept of utilizing mixtures of compounds that may interfere with the bacteria QS was recently employed as a unique antipathogenic method. Accordingly, the use of crude plant extracts, with their distinct structural diversity, is regarded as a possible alternative strategy in challenging the growing antibiotic resistance dilemma [7].

The genus *Aloe*, with about 400 species, is the most extensively used plants for ages to alleviate diseases, provide aesthetic benefits, and improve skincare. Despite the numerous species of *Aloe* genus, *Aloe vera* has recently sparked widespread interest among consumers and researchers for its use in cosmetic and pharmaceutical industries [8]. Unfortunately, there is a tendency of mistakenly referring to all species of the genus *Aloe* as *Aloe vera*, despite the diversity of aloes in the region. The names for the different *Aloe* species in local languages are usually the same for the different species [9]. In traditional medicine, some *Aloe* species are used as remedies for infectious diseases in Egypt, China, and India [9–12]. *Aloe marlothii* (Mountain Aloe) is traditionally used in the treatment of roundworm infestations, stomach, and respiratory disorders, while *Aloe striata* (Coral Aloe) is used to treat rheumatism and leg pain [11]. Despite their usage in traditional medicine, few reports were traced concerning their phytochemical profiles and biological activities. The investigated species exhibited significant pharmacological properties including antimicrobial, hepatoprotective, anti-inflammatory, antioxidant, antiproliferative, moisturizing, and skin protection [13–22].

Here, we hypothesize that the effectiveness of the two investigated species against *P. aeruginosa* may underlie their traditional uses in the control of intestinal, lung and musculoskeletal ailments. Therefore, we evaluated the anti-virulence activities of leaves and roots of *A. marlothii* and *A. striata* against *P. aeruginosa* as well as performed a comparative chemical profile via HPLC–PDA-MS/MS analysis combined with computational analysis to get insight into the marker compounds responsible for the bioactivity.

Materials and methods

Plant material and extraction

Aloe marlothii A. Berger (AM) and *Aloe striata* Haw (AS) were collected from Helal Cactus Farm (Al-Mansouria, Giza, Egypt) in August 2021 in compliance with the institutional, national, and international guidelines and legislation (ARRIVE guidelines). The plant taxa were checked and confirmed on https://wfoplantlist.org/. The leaves and roots of each species were separated, dried, and finely ground. The powdered plants' material (500 g each) was separately extracted twice using 2 L of methanol at ambient temperature. Solvent extracts were filtered, and the combined filtrates (for each extract) were evaporated in a rotary evaporator at 50 °C until completely dryness to yield 22.23 g, 18.23 g, 20.29 g, and 17.96 g dried extracts of *A. marlothii* leaves (AML), *A. marlothii* roots (AMR), *A. striata* leaves (ASL), and *A. striata* roots (ASR), respectively.

Bacterial strains and media

The tested extracts (AML, AMR, ASL, and ASR) were primarily screened for their antimicrobial activity against *Staphylococcus aureus*, *Pseudomonas aeruginosa*, *Klebsiella pneumoniae*, *Enterococcus faecalis,* and *Candida albicans*. The overnight cultures were made from -80 °C frozen culture stocks in a nutrient-rich Luria–Bertani (LB) broth (Oxoid, USA) at 37 °C while being shaken at

180 rpm. To test the motility of *P. aeruginosa* isolates, the swimming media (1% tryptone, 0.5% NaCl, and 0.5% agar) and the swarming media (0.5% peptone, 1% glucose, 0.2% yeast extract, and 0.5% agar) were used. The pyocyanin test was conducted using King A broth (peptone 2%, K_2SO_4 1.0%, and $MgCl_2$ 0.14%).

Antibacterial activity

Agar well-diffusion assay

The antibacterial activity of the examined substances was assessed using the agar well-diffusion method against yeast (*C. albicans* ATCC 90028), Gram-positive bacteria (*S. aureus* ATCC 43300 and *E. faecalis* ATCC29212), and Gram-negative bacteria (*P. aeruginosa* ATCC 27853 and *K. pneumoniae* ATCC 27853). Briefly, a well (6 mm) was previously prepared on Mueller–Hinton agar medium (Oxoid, USA) and streaked with bacterial species. A volume of 100 µL of each extract (5 mg/mL) was added to the well (0.5 McFarland). For 24 h, the inoculation plates were incubated at 37 ± 2 °C. Each well's inhibitory zone was assessed and recorded in millimeters. The imipenem (Imp.) well (256 µg/mL) was used as a positive control [23].

Determination of minimum inhibitory concentrations (MIC)

The MIC of the studied extracts was performed using the broth microdilution technique. Each extract was serially diluted and received an inoculum of a pure bacterial species equating to a 0.5 McFarland standard in Mueller–Hinton broth with or without extract, which was then incubated at 37 °C for 24 h [24]. Then, each well of the 96 wells received 5 µL of the indicator resazurin dye, which was created by dissolving 0.016 g in 100 mL of sterile distilled water. Examining the color change after the incubation time (4–24 h) revealed that a shift from purple to pink or colorlessness is a clear sign of bacterial metabolic activity. The lowest concentration at which the color change took place was identified as the MIC value. With an average of three results, the MIC of the test material and the bacterial strain were computed [25].

Evaluation of the anti-virulence activity of the extracts

The impact of the examined extracts on *P. aeruginosa* motility, pyocyanin, and biofilm was assessed. Results were documented using the sub-MICs of the substances that had been examined.

Biofilm assay

According to [26], the microtiter plate (MTP) technique was used in 96-well flat-bottom polystyrene microtiter plates to measure the investigated extracts' biofilm-inhibiting efficacy. Briefly, each well was filled with 200 µL of bacterial suspension in trypticase soy broth with 1% glucose equivalent to 0.5 McFarland after a further 1:100 dilution with a fresh medium and control organism with and without sub-MICs of investigated extracts. The plate was then incubated for 24 h at 37 °C. After that, each well was rinsed three times with 300 µL of phosphate buffer saline and mild tapings. The remaining adhering bacteria were heat fixed by heating them at 60 °C for 60 min. A 150 µL dose of crystal violet dye was placed in each well. Following the removal of the excess stain, the plate was cleaned after 15 min. After adding 150 µL of 95% ethanol to each well, the OD of the stained, adhering bacterial films was measured at 492 and 630 nm after 30 min. The test was run three times, and the average of the findings was calculated. The percentage (%) of bacterial biofilm inhibition was calculated using the equation [(Ac-At)/Ac] 100, where Ac represents the average of six replicates of the negative controls' light absorption values at 492 nm and 630 nm and At represents the average of six replicates of the samples' light absorption values at 492 nm and 630 nm. PAO1 was used as a positive control for biofilm formation [27].

Pyocyanin assay

Pyocyanin was quantified using King A broth (peptone 2%, K_2SO_4 1.0%, and $MgCl_2$ 0.14%) in triplicate. With and without sub-MICs of the investigated drugs, a 500 µL overnight *P. aeruginosa* culture was inoculated into 5 mL of King A medium and cultured for 24–48 h at 37 °C [28, 29]. Pyocyanin (a green pigment) was extracted with $CHCl_3$ (3 mL), to which 1 mL of HCl 0.2 N was added to produce a pink tint. The solution's OD520 nm reading was then taken. Pyocyanin concentration was given as µg/mL (OD 520 17.072). Each test was carried out in triplicate. PAO1 was used as a positive control for pyocyanin formation.

Motility assay

P. aeruginosa is a motile bacterium that may swarm on semisolid surfaces, streaked on hard surfaces, and swim on soft surfaces [29]. Isolates were diluted from an overnight culture to 0.1–0.2 nm at OD600. Swimming media were used to test flagellum-dependent swimming, and swarming media were used to test swarming motility. After adding 2 µL of 0.5 McFarland *P. aeruginosa* to the plates, they were incubated at 37 °C for 24 and 48 h with and without sub-MICs of the investigated drugs. A measurement of the turbid zone's diameter (mm) was made [30, 31]. The motility experiment was carried out three times, and the mean diameter was computed. PAO1 was used as a positive control for swimming and swarming motility assay.

HPLC–MS/MS analysis

The methanolic extracts of *A. marlothii* (AML and AMR) and *A. striata* (ASL and ASR) leaves and roots (10 mg, each) were separately dissolved in methanol (1 mL), centrifuging at 13,000 × g for 10 min, and filtering through a 0.22 m syringe nylon filter before being used for metabolic analysis. A Shimadzu LC–MS 8050 (Shimadzu, Japan) LC system utilized with a triple quadruple spectrometer and outfitted with autosampler (SIL-40C xs) was used in negative ionization mode according to [32]. A triple quadruple spectrometer with an ESI source was utilized. Separation was performed on a C18 reversed-phase column (Zorbax Eclipse XDB-C18, rapid resolution, 4.6 × 150 mm, 3.5 µm, Agilent, Santa Clara, CA, USA) with a flow rate of 1 mL/min, and gradients of water and acetonitrile (ACN) containing 0.1% formic acid each were used from 5 to 30% ACN over the course of 60 min and then increased to 90% over the last 20 min. The device was operated by Shimadzu's (Japan) LC solution software. The MS was in a negative phase of operation.

Docking study

Molecular docking was performed using in silico drug design tools according to the previously described method [88] and by applying the parameters of AMBER10:EHT forcefield. The co-crystal structure of LasR with TP-4 was obtained from the Protein Data Bank (PDB: 3JPU) available at http://www.rcsb.org/pdb. Protein preparation was carried out to correct the errors in protein structure, add hydrogens, and calculate partial charges. The binding pocket was isolated, and the energy-minimized ligands were docked using the triangle matcher placement method. Final poses were ranked using GBVI/WSA dG scoring function. The 2D interaction diagram for each ligand was generated using the Ligand Interactions tool in the software.

Statistical analysis

Statistical analyses were conducted through one-way analysis of variance (ANOVA) followed by Dunnett's multiple comparisons test. The statistical assessments were conducted using Graph Pad Prism v. 8.0 (GraphPad Software, Inc., CA, USA), considering significance when the p value is ≤ 0.05.

Results

Antimicrobial activity and MIC determination

The in vitro antibacterial abilities of the extracts were examined in the current study against both Gram-positive and Gram-negative bacteria. By measuring the presence of an inhibitory zone and the width of the zone, the extracts' potency and antibacterial activity were quantitatively evaluated. As shown in Table 1, only *P. aeruginosa* was significantly inhibited by AML, AMR, and ASL.

Evaluation of the anti-virulence activity of the extracts

Antibiofilm activity

The current study evaluated the impact of the AML, AMR, and ASL extracts at sub-MIC levels (0.5 × MIC and 0.25 × MIC concentrations) on *P. aeruginosa's* development of biofilm, for the first time. Interestingly, ASL decreased biofilm formation in a dose-dependent manner (37.0% at 0.25 MIC and 46.4% at 0.5 MIC), while AMR decreased the biofilm 19.0% at 0.5 MIC but no inhibition was observed by AML at both tested doses, compared to PAO1 (Fig. 1).

Anti-pyocyanin activity

The impact of AML, AMR, ASL, and ASR at sub-MIC levels on *P. aeruginosa's* synthesis of pyocyanin was assessed. The pyocyanin production was decreased by 75% and 70% by AMR and ASL, respectively, while AML and ASR did not affect this pigment, compared to PAO1 (Fig. 2).

Table 1 The antibacterial activity and the MIC of AML, AMR, ASL, and ASR extracts

Sample	Zone mm					MIC mg/mL
	S	P	K	C	E	P
AML	–	14.5	–	–	–	3.0
AMR	–	12.3	–	–	–	3.0
ASL	–	10.7	–	–	–	1.0
ASR	–	–	–	–	–	–
Imp	40	15	–	–	–	–

AML: *A. marlothii* leaves; AMR: *A. marlothii* roots; ASL: *A. striata* leaves; ASR: *A. striata* roots; (Imp.): Imipenem, S: *S. aureus*, P: *P. aeruginosa*, K: *Klebsiella pneumoniae*, C: *Candida albicans,* and E: *Enterococcus faecalis*

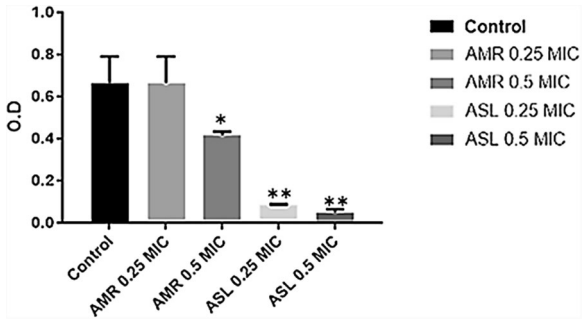


Fig. 1 The effect of sub-MIC of AMR and ASL extracts on biofilm formation. AMR: *A. marlothii* roots; ASL: *A. striata* leaves**.** The results are expressed using the means ± S.E.M., $n = 6$. Statistical analysis was done using one-way ANOVA, followed by Dunnett's multiple comparisons test. (*) indicates p value < 0.01, and (**) indicates p value < 0.0001 compared with the positive control group (PAO1)

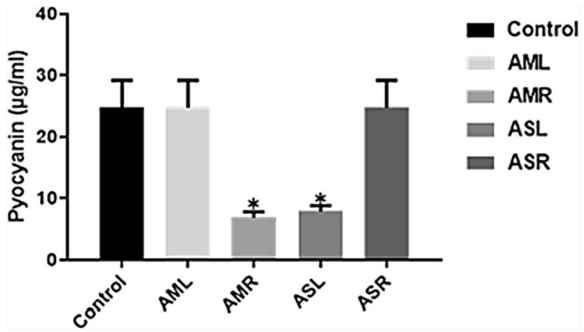


Fig. 2 The effect of sub-MIC of AML, AMR, ASL, and ASR extracts on pyocyanin production. AMR: *A. marlothii* roots; ASL: *A. striata* leaves**.** The results are expressed using the means ± S.E.M., $n = 3$. Statistical analysis was done using one-way ANOVA, followed by Dunnett's multiple comparisons test. (*) indicates p value < 0.0001 compared with the positive control group (PAO1)

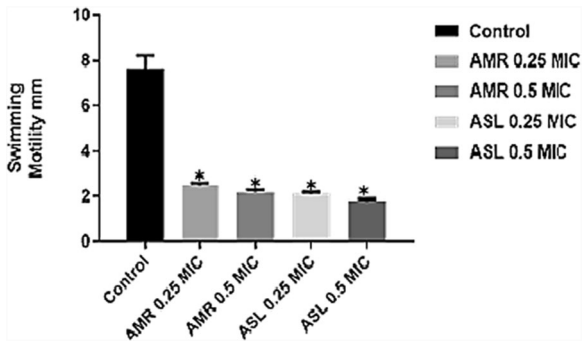


Fig. 3 The effect of sub-MIC of AMR and ASL extracts on swarming motility. AMR: *A. marlothii* roots; ASL: *A. striata* leaves**.** The results are expressed using the means ± S.E.M., $n = 3$. Statistical analysis was done using one-way ANOVA, followed by Dunnett's multiple comparisons test. (*) indicates p value < 0.0001 compared with the positive control group (PAO1)

Anti-motility activity

After treatment with sub-MIC (0.25 and 0.5 MIC) of AMR, the swarming and swimming motility was decreased by 68.75% and 72.5%, respectively (Fig. 3). ASL at 0.25 mg/mL and 0.5 mg/mL decreased the swarming and swimming by 73.8% and 77.5%, respectively, compared to PAO1 (Fig. 3), while treatment with sub-MIC (0.25 and 0.5) of AML and ASR did not affect the swarming and swimming motility of *P. aeruginosa,* compared to PAO1.

HPLC–MS/MS analysis

Metabolites were characterized by their retention time, MS data (mass and MS/MS spectra). Identification of the metabolites was confirmed by comparison with the Phytochemical Dictionary of Natural Product Database (https://dnp.chemnetbase.com/faces/chemical/ChemicalSearch.xhtml)and LipidMaps (https://www.lipidmaps.org/). In addition, the diagnostic MS/MS fragments, ionization behavior, and reviewing of the documented chemical profile of genus *Aloe* [20, 33–39] provided additional support for the compound annotations. In total, 100 compounds were identified in the extracts. These compounds belong to different chemical classes, including sugars, organic acids, amino acids, nucleosides, phenolic acids, chromones, phenyl pyrones, flavonoids, anthrones/anthraquinones and lipids. The details on their masses $[M\text{-}H]^-$, molecular formulas, retention time, tentative identification, and chemical class in the four samples are shown in Table 2 **and** Fig. 4. The detected metabolites' structural elucidation is outlined in the paragraphs that follow.

Identification of Sugars and sugar acids

Results revealed the presence of 2 sugar acids (1 and 3) and 2 sugars (2 and 4) which were characterized by loss of H_2O (-18 Da) molecules [7]. The disaccharide (4) showed loss of hexose moiety (-162 Da). Hexuronic acid (1) was only detected in the leaves of both species.

Identification of organic acids

Three organic acids (5–7), namely malic, citric and quinic, were detected in the extracts. Decarboxylation (−44 Da) and water elimination (−18 Da) were detected in their fragmentation pattern [40]. The organic acids were detected in all the tested extracts.

Identification of amino acids and nucleosides

Seven amino acids were tentatively identified, including pyroglutamic acid (9), m-carboxyphenyl-L-alanine (11), tryptophan (15), alongside glycosides as hexosyl pyroglutamic acid (8), hexosyl isoleucine (10), hexosyl

Table 2 Compounds identified in the methanol extracts of *Aloe marlothii* and *Aloe striata* (leaves and roots) by HPLC–PDA-MS/MS analysis

No	Rt (min)	$[M-H]^-$	MS/MS (m/z)	Identification	AML	AMR	ASL	ASR
Sugars and sugar acids								
1	1.30	193	85, 73, 71, 59	Hexuronic acid	+	–	+	–
2	1.41	179	151, 131, 120	Hexose	+	+	+	+
3	1.94	195	129, 115	Gluconic acid	+	+	+	+
4	7.69	341	179, 133	Disaccharide	+	+	+	+
Organic acids								
5	1.31	133	115	Malic acid	+	+	+	+
6	1.47	191	111	Citric acid	+	+	+	+
7	1.91	191	172, 155, 129	Quinic acid	+	+	+	+
Amino acids and nucleosides								
8	2.03	290	128	Hexosyl pyroglutamic acid	–	+	–	–
9	2.11	128	111, 93	Pyroglutamic acid	+	+	+	+
10	2.33	292	130, 101	Hexosyl isoleucine	+	+	+	–
11	2.48	208	164	m-Carboxyphenyl-L-alanine	+	–	+	–
12	2.64	266	134	Adenosine	–	+	–	+
13	2.83	282	150	Guanosine	+	+	–	–
14	4.32	326	164, 147	Hexosyl phenylalanine	+	+	+	–
15	6.57	203	144, 130, 116	Tryptophan	+	+	+	+
16	9.91	293	131	Hexosyl asparagine	+	+	+	+
Phenolic acids and their derivatives								
17	2.78	311	179, 149, 135	Caftaric acid	+	+	+	–
18	6.22	153	109	protocatechuic acid	+	+	+	+
19	6.82	515	191 178, 161	Dicaffeoyl quinic acid	+	–	–	+
20	6.90	515	323, 191, 135	Caffeoylquinic acid hexoside	+	–	–	–
21	6.93	183	168, 125	Methyl gallate	+	+	+	–
22	7.43	353	191, 179	3-*O*-Caffeoylquinic acid (neochlorogenic acid)	+	+	+	–
23	7.70	367	193, 134	3-*O*-Feruloylquinic acid	+	+	+	–
24	9.17	137	118, 109	protocatechualdehyde	+	–	+	+
25	11.55	325	145, 117	Coumaric acid glucoside	+	+	+	–
26	11.87	353	191, 127	5-*O*-Caffeoylquinic acid (chlorogenic acid)	–	+	–	–
27	12.12	353	191, 173, 135	4-Caffeoylquinic acid (cryptochlorogenic acid)	+	+	+	–
28	13.05	179	135	Caffeic acid	+	+	+	+
29	13.10	197	169, 125	Ethyl gallate	–	–	+	+
30	15.81	337	191, 173, 118	Coumaroylquinic acid	+	+	+	+
31	16.75	335	161, 135	Caffeoylshikimic acid	–	+	+	–
32	17.60	367	193, 191, 173	4-*O*-Feruloylquinic acid	–	–	+	–
33	17.61	367	193, 191, 173	5-*O*-Feruloylquinic acid	+	+	+	+
34	19.40	193	178, 134	Ferulic acid	+	+	+	+
35	23.61	623	461, 315, 179	Verbascoside	–	–	+	–
36	31.57	529	367, 353	3-*O*-(E)-caffeoyl-4-*O*-feruloylquinic acid	+	+	–	+
Chromone								
37	7.24	353	233, 205	Undulatoside A	–	+	–	–
38	10.67	393	273, 245, 203	Aloesin	+	+	+	+
39	22.55	395	275, 231, 203	Aloesol-C-glucosyl	+	+	+	+
40	27.16	539	375, 285, 163	Coumaroyl aloesin	+	–	–	+
41	28.23	569	375, 285, 193	Aloesin-O-feruloyl	+	–	+	–
42	29.70	555	513, 438, 273	Isoaloeresin D	+	–	–	–
43	30.32	189	147	Altechromone A	–	+	+	+

Table 2 (continued)

No	Rt (min)	$[M-H]^-$	MS/MS (m/z)	Identification	AML	AMR	ASL	ASR
44	35.41	407	287, 259	Methyl aloesin	+	–	–	–
45	60.54	583	570, 407, 272	Feruloyl aloesin methyl ether	–	+	–	–
Phenyl pyrones								
46	18.94	717	409, 307, 247	Aloenin B	+	+	–	–
47	23.23	555	247, 391, 307	Coumaroylaloenin	+	+	+	–
48	28.52	571	409, 247	Glucopyranosyl aloenin	+	+	–	+
49	71.01	409	307, 247	Aloenin	+	–	–	–
Flavonoids								
50	16.72	593	503, 383, 353	Apigenin-6,8-C-diglucoside (vicenin II)	–	+	–	–
51	18.62	609	327	Luteolin-C-hexoside-*O*-hexoside	+	–	+	–
52	19.26	579	459, 447, 285	Luteolin-C-hexoside-*O*-pentoside	+	–	–	–
53	19.95	447	357, 327, 285	Luteolin-6-C-glycoside (isoorientin)	–	–	–	+
54	20.14	447	357, 327, 285	Luteolin-8-C-glycoside (orientin)	+	+	+	+
55	23.33	463	301	Isoquercitrin	+	+	–	+
56	24.17	593	431, 311,297	Apigenin-C-hexoside-O-hexoside	+	–	–	–
57	25.13	461	371, 341, 285	Luteolin-methoxy-C-hexoside	+	–	–	–
58	25.02	447	227	Kaempferol-O-hexoside	+	+	+	+
59	29.32	447	285	Luteolin O-hexoside	–	+	+	–
60	29.33	747	482	Wighteone-O-diglucoside malonylate	–	+	+	+
61	31.49	431	341, 311	Isovitexin (apigenin-6-C-glycoside)	+	+	+	+
62	36.86	431	341, 311	Vitexin (apigenin-8-C-glycoside)	+	+	+	+
63	40.26	477	315, 285, 243	Isorhamnetin-O-glucoside	+	–	–	–
64	41.15	343		Eupatorin	+	+	+	+
Anthrones								
65	23.25	433	343, 313, 271	10-Hydroxyaloin B	–	+	+	–
66	24.99	447	285, 269	8-O-Methyl-7-hydroxyaloin B	+	+	+	+
67	26.00	433	343, 313, 271	10-Hydroxyaloin A	–	+	+	–
68	26.12	433	396, 342, 271	5-Hydroxyaloin A	–	+	+	–
69	27.21	593	269	Aloe-emodin diglucoside	+	–	+	+
70	28.94	593	269	Aloe-emodin diglucoside isomer	+	–	+	+
71	29.27	447	285, 269	8-O-methyl-7-hydroxyaloin A	+	+	+	+
72	31.91	417	297, 268, 255	Aloin B (isobarbaloin)	–	+	+	+
73	32.82	297	238, 208	Dimethyl ether of *Aloe*-emodin	–	+	+	+
74	33.66	563	443, 297	Aloinoside A/B	–	–	+	
75	33.95	417	297, 268, 239	Aloin A (Barbaloin)				
76	36.90	503	297, 268	6′-Malonylnataloin	+	+	–	–
77	39.98	415	253	Chrysophanol-8-*O*-glucoside	–	+	+	–
78	41.74	431	269	Aloe-emodin-8-*O*-glucoside	+	+	+	+
79	46.54	315	297, 285, 256	Aloesaponol I	–	+	–	+
80	55.94	269	240, 223, 196	Aloe-emodin	+	+	+	+
81	58.21	311	223, 195	Aloesaponarin I	–	+	–	+
82	58.82	253	225	Chrysophanol	–	+	+	–
83	59.75	283	240, 212	Physcion				+
84	59.78	283	183, 169	Rhein	+	+	–	–
Lipids								
85	51.55	255	211, 196	Palmitic acid	–	–	–	+
86	59.84	476	279, 140	LPE 18:2	+	+	+	+
87	60.48	564*	279, 242, 224	LPC 18:2	+	+	+	+
88	61.26	452	255, 196, 140	LPE 16:0	+	+	+	+

Table 2 (continued)

No	Rt (min)	$[M-H]^-$	MS/MS (m/z)	Identification	AML	AMR	ASL	ASR
89	61.59	595	415, 315, 241	LPI 18:2	+	+	–	+
90	62.27	540*	255, 224	LPC 16:0	+	+	+	+
91	63.55	571	255, 241, 153	LPI 16:0	+	+	+	+
92	63.83	297	183	Hydroxy oleic acid	+	+	+	+
93	65.10	695	279, 153	PA (18:2/18:2)	–	–	–	+
94	65.30	325	237, 121	Trihydroxy octadecatrienoic acid	+	+	+	+
95	65.60	671	279, 255, 153	PA (16:0/18:2)	–	–	–	+
96	66.13	311	183	Octadecatrienoic acid	+	+	+	+
97	66.96	433	279, 171, 153	LPA (18:2)	+	+	–	+
98	70.74	409	255, 171, 153	LPA 16:0	+	+	+	+
99	70.86	833	279, 255, 241	PI (16:0/18:2)	–	+	–	–
100	71.92	327	183	Hydroxy eicosanoic acid	+	+	+	+

AML: *A. marlothii* leaves; AMR: *A. marlothii* roots; ASL: *A. striata* leaves; ASR: *A. striata* roots; LPA: lysophosphatidic acid; LPC: lysophosphatidylcholine; LPE: lysophosphatidylethanolamine; LPI: lysophosphatidylinositol; R_t, retention time; PI, phosphatidylinositol; and PA, phosphatidic acid, *: $[M+HCOO]^-$

phenylalanine (14), hexosyl asparagine (16). The glycosides showed the same fragmentation pattern losing the attached sugar (−162 Da) and base peak formation at *m/z* 128, 130, 164, 131 for compounds 8, 10, 14, and 16, respectively [40]. Nearly, all the studied extracts showed similar amino acids except for hexosyl pyroglutamic acid (8) were detected in AMR, hexosyl isoleucine (10) and hexosyl phenylalanine (14) were absent in ASR and m-carboxyphenyl-L-alanine (11) was detected only in the leaves extracts. In addition, 2 nucleosides were detected [adenosine (12) and guanosine (13)].

Identification of phenolic acids and their derivatives

A total of 20 phenolic acids and their derivatives (17–36) were tentatively identified in the extracts. They were mainly hydroxycinnamic and benzoic acids derivatives. Fifteen hydroxycinnamic acid derivatives were identified. They are mainly represented by esters of quinic or shikimic acids condensed either with caffeic, ferulic, or coumaric acids. Those compounds displayed characteristic fragment ions corresponding to quinic, ferulic, coumaric, and caffeic acids at *m/z* 191, 193, 163, and 179, respectively [36, 41]. Regarding compounds 22, 25, and 26, they showed the same $[M-H]^-$ at *m/z* 353, yielding fragments at *m/z* 191, 179, 173, and 135 on MS/MS spectra, which are characteristic fragments of caffeoylquinic acids [quinic acid-H]$^-$, [caffeoyl-H]$^-$, [quinic acid-H-H_2O]$^-$, [caffeoyl-H-COO]$^-$, respectively. Compounds (22 and 25) both yielded base peak at *m/z* 191 and were identified as 3-*O*-caffeoylquinic acid (neochlorogenic) and 5-*O*-caffeoylquinic acid (chlorogenic acid), respectively, based on the relative abundance of the peak at *m/z* 179 [42]. Compound 26 was identified as 4-*O*-caffeoylquinic acid (cryptochlorogenic acid) due to the distinctive base peak at m/z 135 and the abundant fragment ion at *m/z* 173 [35, 42]. Both compounds 19 and 20 yielded pseudomolecular ion at *m/z* 515 which was 162 Da higher than compounds (22, 25, and 26). They showed diagnostic fragmentation (m/z 191, 179, and 135) of caffeoylquinic acids. Thus compound 19 could be identified as di-caffeoylquinic acid. However, compound 20 showed distinctive ions at *m/z* 323 ([caffeoyl hexoside – H – H_2O]$^-$) characteristic for caffeoylquinic acid hexoside which was not detected in compound 19 [43]. Compounds 23, 32, and 33 gave pseudomolecular ions at *m/z* 367 that gave rise to fragment ions at *m/z* 193 characteristic to feruloyl moiety [ferulic acid – H]$^-$ and *m/z* at 191 [quinic acid – H] –, and 173 [quinate – H_2O]$^-$ corresponding to quinic moiety. They were identified according to their characteristic fragmentation [44]. Compound 35 detected in ASL exhibited loss of sugar moiety yielding fragment ion at *m/z* 416 (-162 Da) and characteristic fragment ion of phenylpropanoid moiety at *m/z* 161 [caffeic acid-H-H_2O]$^-$. The compound was identified as the phenylethanoid verbascoside [45]. It is reported for the first time in *Aloe* species. Four benzoic acid derivatives were detected: protocatechuic acid (18), methyl gallate (21), protocatechualdehyde (24), and ethyl gallate (29). They showed loss of CO_2 (44 Da) and CO (28 Da) groups which are characteristic fragmentation pattern of phenolic acids [46].

Identification of chromones

Nine chromones were tentatively identified (37–45). Chromone-*O*-glycosides were detected as undulatoside A (37) that showed fragment ions at *m/z* 233 and 205 due to loss of $C_4H_8O_4$ and $C_5H_8O_5$, respectively [47]. The majority of the detected chromones were C-glycosylated that

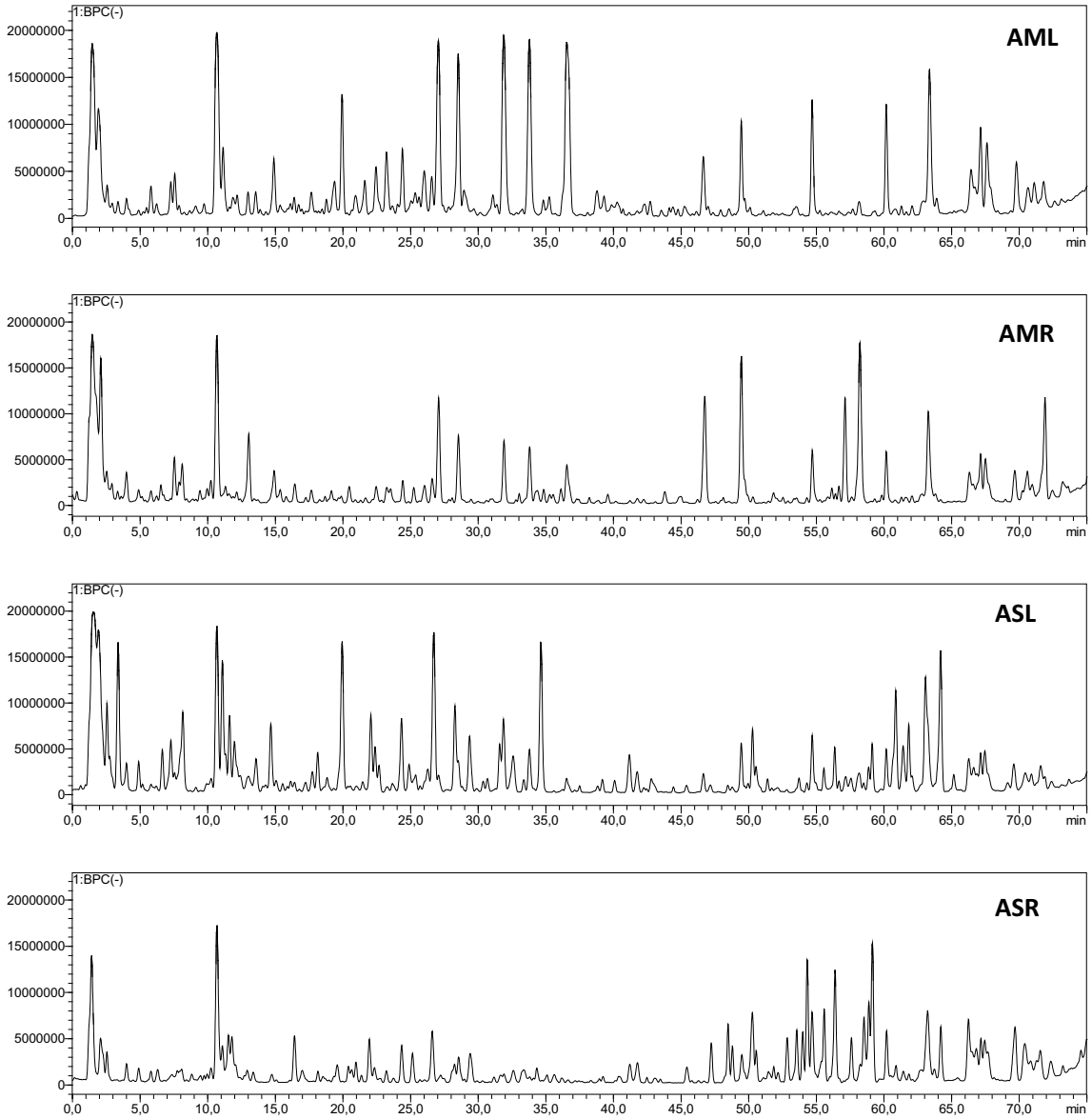


Fig. 4 LC chromatogram of methanolic extracts of *A. marlothii* and *A. striata* leaves and roots. AML: *A. marlothii* leaves; AMR: *A. marlothii* roots; ASL: *A. striata* leaves; and ASR: *A. striata* roots

are distinct components of *Aloe* species and not reported in other plant species [48]. The MS/MS of the C-glycosylated chromones as aloesin (38) and methyl aloesin (44) showed a diagnostic loss of 120 Da which is characteristic for C-glucosides [38]. It was detected only in AMR. It was identified as the chromone glycoside, undulatoside A which was previously reported in *A. vera* leaves [35]. The chromone derivative, altechromone A (43), showed fragment ion at m/z 146 $[M\text{-}H\text{-}CH_3\text{-}CO]^-$ [49].

Identification of phenyl pyrones

Four phenyl pyrones were identified: aloenin B (46), coumaroylaloenin (47), glucopyranosyl aloenin (48), and aloenin (49). The MS/MS of aloenin (49) showed fragment ion at *m/z* 307 due to loss of $C_4H_6O_3$ and a distinct fragment ion at *m/z* 247 representing the phenyl pyrone aglycone [50]. Phenyl pyrones have a limited distribution in *Aloe* species, with aloenin restricted to few *Aloe* species [51]. Herein, aloenin was detected in AML.

Identification of flavonoids

Flavonoid glycosides represent a prevalent class in *Aloe* species. Herein, 15 flavonoids were determined. They were detected as trimethoxy flavone, C-glycosylated flavones *O*, C-di-glycosylated flavones, *O*-glycosylated, and malonylglucoside isoflavone. Flavones were the most frequent subclass where apigenin and luteolin with various sugar attachments were detected. Flavonols were the second subclass determined in the studied *Aloe* species. The fragmentation of flavones di-C-glycosides was observed in apigenin-6,8-C-diglucoside (vicenin II) (50) showing loss of 90 Da (*m/z* 503) and 210 Da (*m/z* 210) [52], while that of mono-C-glycosylated flavones was observed in luteolin-6-C-glycoside (isoorientin) (53) and luteolin-8-C-glycoside (orientin) (54) showing loss of 90 Da (*m/z* 357) and 120 Da (*m/z* 327). However, the higher abundance of $[M\text{-}H\text{-}90]^-$ over that of $[M\text{-}H\text{-}120]^-$ confirmed the 6-C-glyco assumption and vice versa [52]. Regarding *O*, C-di-glycosylated flavones, luteolin-C-hexoside-*O*-pentoside (52) showed loss of 132 Da (*m/z* 447) confirming the presence of C-pentose. It also exhibited characteristic fragmentation of C-hexoside represented by the loss of 120 Da due to cross-ring cleavage (O-C1). As an example of *O*-glycosylated flavonoid, luteolin *O*-hexoside (59) showed loss of hexosyl moieties (-162 Da).

Identification of anthrones and anthraquinones

Ten C-glycosylated anthrones were characterized (65–76). Their mass spectra displayed the characteristic fragmentation of C-glycosides (loss of $C_4H_8O_4$) represented by $[M\text{-}H\text{-}120]^-$ fragment ions. Compounds 72 and 75 were identified as two isomers showing fragment ions at *m/z* 297 due loss of (-120 Da) followed by further loss of CHO yielding fragment ions at *m/z* 268 $[M-H-120-CHO]^-$ and *m/z* 239 $[M-H-120-2CHO]^-$ [33, 50]. Aloinoside A/B (74) is the *O*-rhamnoside of aloin A/B which showed fragment ions at *m/z* 443 $[M-H-120]^-$ and at *m/z* 297 due to the subsequent loss of rhamnosyl moiety (−146 Da) [53]. 6′-Malonylnataloin (76) showed a base peak at *m/z* 297 due to the concomitant loss of $C_4H_8O_4$ (−120 Da) and malonyl (-86 Da) [35]. 10-Hydroxyaloin B (65), 10-hydroxyaloin A (67), 5-hydroxyaloin A (68), aloin A (75), and 6′-malonylnataloin (76) were detected in AMR and ASL only. Anthraquinone aglycones were detected as well (73, 79–84). Aloe-emodin (80) produced a characteristic fragment ions at *m/z* 240 $[M–H–CHO]^-$. It is a characteristic constituent of *Aloe* species [54]. It was detected in the four tested extracts. Aloesaponarin I (81) showed fragment ions at 225, 195 due to loss of CH_3OH-2CO and CH_3OH-3CO, respectively. Aloesaponol I (79) and aloesaponarin I (81) were detected in the roots of both species. Chrysophanol (82) was determined in AMR and ASL only. Aloe-emodin glycosides were detected [aloe-emodin diglucoside (69), aloe-emodin diglucoside isomer (70), aloe-emodin-8-*O*-glucoside (78)] having diagnostic ions at *m/z* 269 [49]. Compound 77 was detected in AMR and ASL and determined as chrysophanol-8-*O*-glucoside showing diagnostic ion at *m/z* 253 [49].

Identification of lipids

Four fatty acids [palmitic acid (85), hydroxy oleic acid (92), trihydroxy octadecatrienoic acid (94), and octadecatrienoic acid (96)] were identified as well as 12 phospholipids were identified. Lysophosphatidylcholine (LPC) [LPC 18:2 (87) and LPC 16:0 (90)] formed primarily $[M+HCOO]^-$ and the rest of the lipids tended to render $[M\text{-}H]^-$ (Table 2). Diagnostic fragment ion at *m/z* 140 for deprotonated ethanolamine appeared in 86 and 88 justifying their nature as lysophosphatidylethanolamine (LPE) [55]. LPE 16:0 (86) showed fragments ions at *m/z* 196 and 255 which detected the loss of ketene $[C_5H_{11}NO_5P]^-$ and fatty acyl chain (16:0) [56], while a prominent fragment ion at m/z 279 was detected in LPE 18:2 (88) corresponding to fatty acyl chain (18:2). A characteristic fragment of the inositol headgroup of phosphatidylinositol (PI) $[C_6H_{10}O_8P]$- at *m/z* 241 [57] and fragment ion at m/z 415 due to neutral loss of inositol from the pseudomolecular ion were detected in lysophosphatidylinositol (LPI 18:2) (89), LPI 16:0 (91), and PI 16:0/18:2 (99). In addition to prominent fragment ions at *m/z* 279 and *m/z* 255 were detected characteristic for fatty acyl chain (18:2) and (16:0) [56]. Phosphatidic acids [PA 18:2/18:2 (93) and PA 16:0/18:2 (95)] and lysophosphatidic acid [LPA 18:2 (97) and LPA 16:0 (98)] were characterized by the presence of a diagnostic fragment ion m/z 153 glycerol-3-phosphate after loss of water [55]. Also, fragment ions were determined as carboxylate anions at *m/z* 255 and 279, corresponding to fatty acid 16:0 and 18:2.

Molecular docking of anthraquinone compounds from *A. marlothii* and *A. striata* extracts

AMR and ASL displayed significant anti-virulence activity against *P. aeruginosa*. Anthrones and anthraquinones are a marker for *Aloe* species, and docking of identified anthrones and anthraquinones was performed to predict the binding mode of these compounds to LasR target (Table 3). The docking protocol was first validated by redocking of the co-crystallized compound TP-4 that showed a docking score (S) of −10.67 kcal/mol and RMSD of 0.19. Compound TP-4 forms three H-bond interactions with LasR residues Asp73, Tyr56, and Ser129, in addition to, a pi–pi interaction with residue Tyr64 (Fig. 5A). These residues are pivotal in determining the potential

Table 3 Docking scores and interaction residues of the docked compounds

No	Compound	Interactions	Docking score S (kcal/mol)
	TP-4	ASP73: H-donor; TYR56: H-acceptor; SER129: H-acceptor; TYR64: pi–pi	−10.67
1	Chrysophanol-8-*O*-glucoside	THR75: H-donor; GLY38: H-acceptor; TYR64: pi–pi; TYR64: pi–pi	−9.24
2	6-Malonylnataloin	ASP65: H-donor; ASP65: H-donor; THR75: H-donor; SER129: H-acceptor; TYR64: pi–pi	−9.01
3	Aloe-emodin-8-*O*-glucoside	THR75: H-donor; TRP60: H-acceptor; TRP88: H-pi; TYR64: pi–pi	−8.65
4	Aloin A	ASP65: H-donor; ASP73: H-donor; TYR56: H-acceptor; TYR64: pi–pi	−8.39
5	5-Hydroxyaloin A	ASP65: H-donor; ASP73: H-donor; THR75: H-donor; SER129: H-acceptor; TYR64: pi–pi	−7.50
6	Aloesaponol I	TRP88: H-pi; TYR64: pi–pi	−7.72
7	10-Hydroxyaloin B	ASP65: H-donor; ASP65: H-donor GLY126: H-donor; ASP73: H-donor; THR75: H-donor; TYR56: H-acceptor	−7.72
8	Aloesaponarin I	ASP65: H-donor; THR75: H-donor; TRP88: H-pi; TYR56: pi-H; TYR64: pi–pi; TYR64: pi–pi	−7.75
9	10-Hydroxyaloin A	TYR47: H-donor; ASP65: H-donor; ASP73: H-donor; THR75: H-donor; SER129: H-donor; TYR56: H-acceptor; TRP60: H-acceptor	−6.95
10	Aloe-emodin	ASP73: H-donor; TRP60: H-acceptor; TRP88: H-pi; TYR56: pi-H; TYR64: pi–pi; TYR64: pi–pi	−6.80
11	Chrysophanol	TRP60: H-acceptor; TYR64: pi–pi	−6.15

interaction of compounds with LasR. Most compounds maintained the pi–pi interaction, in addition to, one or more H-bond interactions. Aloin A and 10-hydroxyaloin A interacted with the LasR active site in a comparable mode to TP-4, primarily through H-bonding. Both compounds maintained the H-bond interactions with residues Asp73 and Tyr56, with 10-hydroxyaloin A additionally forming a H-bond with Ser129, similar to the co-crystallized ligand (Fig. 5B and C). Furthermore, aloin A retained the pi–pi interaction with Tyr64. Similar to aloin A, 10-hydroxyaloin B formed H-bonds with Asp73 and Tyr56, while 5-hydroxyaloin A interacted with Asp73 and Ser129 (Table 3). Among the docked compounds, 6-malonylnataloin and chrysophanol-8-*O*-glucoside had the highest docking scores of -9.01 and -9.24 kcal/mol, respectively, binding with LasR through H-bonding and pi–pi interactions (Table 3**,** Fig. 5D and E). However, while both compounds maintained the Tyr64 pi–pi interaction, only 6-malonylnataloin formed a H-bond interaction with Ser129 similar to TP-4. Chrysophanol-8-*O*-glucoside, with a sugar moiety attached to the terminal aromatic ring, adopted a slightly different position in the active site and interacted through a H-bond with Gly38 (Fig. 5E)**.** Less favored binding was observed with chrysophanol that formed a pi–pi interaction with Tyr64 and a H-bond with Trp60 with a docking score of -6.15 kcal/mol (Table 3, Fig. 5F). All compounds engaged with the binding pocket through additional H-bond interactions especially with residues Asp65, Thr75, and Trp60 that formed H-bonds with multiple docked compounds (Table 3). Overall, the compounds bind to the active site of LasR suggesting their potential to inhibit it and promote anti-virulence activity.

Discussion

The increasing demand for the discovery of natural ingredients as antimicrobial agents as an alternative to antibiotics is an emerging research interest nowadays. Previous studies showed the efficacy of *A. marlothii* and *A. striata* against a variety of bacteria [58–61]. In addition, the acetone and aqueous infusion of *A. marlothii* leaves exhibited potential activity against *P. aeruginosa* with MIC values of 0.13 and 0.87 mg/mL, respectively [62]. On the other hand, our study has focused on evaluating the comparative effectiveness of *A. striata* and *A. marlothii* leaves and roots against *P. aeruginosa* for the first time, revealing that *A. marlothii* leaves and roots in addition *A. striata* leaves significantly inhibited the growth of *P. aeruginosa*.

Production of biofilms is a crucial survival strategy for *P. aeruginosa* because they function as a barrier, decreasing the penetration of medications and, as a result, preventing them from exerting their effects [3]. Moreover, pyocyanin is considered as a virulence factor produced by *P. aeruginosa*. It increases the levels of reactive oxygen species and inflammatory cytokines in various organ systems, including the cardiovascular, urological, respiratory, and central nervous systems, leading to fatal diseases [3, 6]. Only AMR and ASL significantly decreased the biofilm formation, pyocyanin production, the swarming and swimming activity in the current investigation. Other studies illustrated the antibiofilm activity of *A. marlothii* leaves against *Clostridium perfringens,* showing

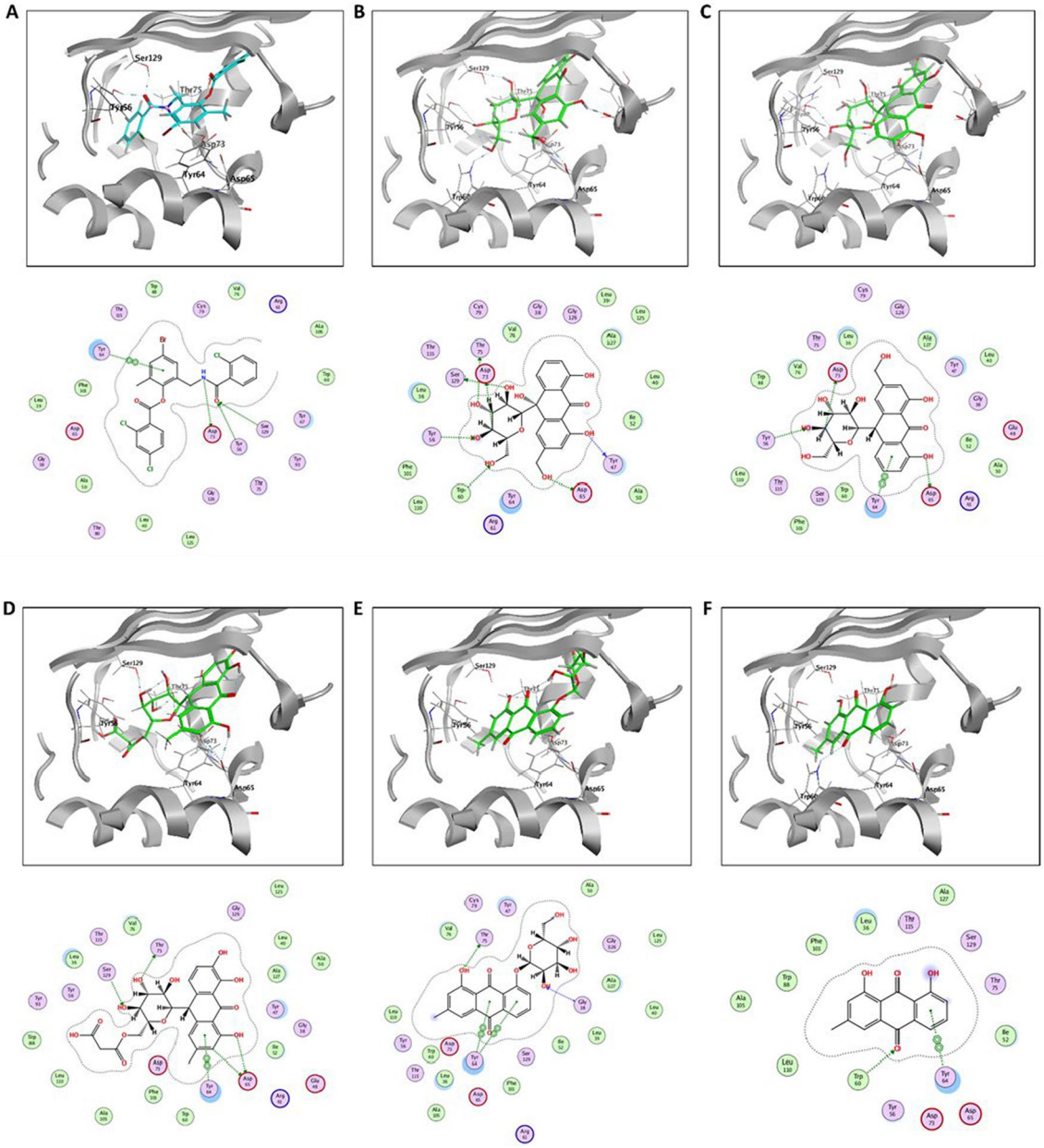


Fig. 5 2D and 3D interactions of the co-crystal compound TP-4 and representative compounds with LasR. **A** TP-4, **B** 10-hydroxyaloin A, **C** Aloin A, **D** 6-malonylnataloin, **E** Chrysophanol-8-*O*-glucoside, and **F** Chrysophanol

potential activity against mature biofilms [63] and the anti-swarming activity of *A. barbadensis* against *P. aeruginosa* [64].

With the aim of identifying the secondary metabolites of *A. marlothii* and *A. striata* that could be responsible for the antibacterial and anti-virulence activities, we performed LC–MS of the AML, AMR, ASL, and ASR extracts. Our findings demonstrated that the examined extracts contain a plethora of bioactive metabolites as phenolic acids, chromones, flavonoids, anthrones, and lipids. Phenolic acids were previously reported to exhibit antibacterial activity [65, 66]. Several *Aloe* leaf components have been linked to antibacterial action. Cinnamic acid, coumaric acid, ascorbic acid, and pyrocatechol isolated from *A. vera* leaves showed strong antibacterial activity, particularly against Gram-positive bacteria [67]. It was proposed that phenolic compounds disrupted bacterial cell membranes and denaturated bacterial proteins. Cinnamic acid inhibited bacterial growth by blocking glucose uptake and ATP generation [68]. Coumaric acid

inhibited various bacterial enzymes [69]. Several phenolic acids showed antibiofilm activity against methicillin resistant *Staphylococcus aureus* [70]. Some phenolic acids as caffeic, cinnamic, and ferulic inhibited the production of QS regulated virulence factors including biofilm formation, pyocyanin production, and swarming motility of *Pseudomonas aeruginosa* [71]. The inhibitory activity of phenolic acids was correlated with the site and degree of hydroxylation that interact with sulfhydryl groups on the proteins [72]. The antimicrobial potentials of aloesin and undulatoside A were previously demonstrated against various bacteria [73–76]. Chromones-based compounds showed potent inhibition of *P. aeruginosa* biofilm [77]. Flavonoids are characterized to exhibit substantial antibacterial activity by providing protection toward plant pathogen, and as a result, they can also demonstrate effectiveness in fighting human pathogens [78]. Flavonoids showed antibacterial activity against *P. aeruginosa* [79]. Anthrones and anthraquinones and pre-anthraquinones are the most important and characteristic constituents of genus *Aloe* [54]. Interestingly, AMR and ASL extracts showed their richness with anthrones in the present study. Aloesaponarin I was previously reported to show antimicrobial activity [80]. Anthrones and anthraquinones are structurally related and have been shown to inhibit growth of several pathogenic microorganisms [81, 82]. The anthrones: 8-*O*-methy-7-hydroxyaloin A/B, aloin A/B isolated from *A. trigonantha,* exhibited pronounced antibacterial activity against various bacteria [74]. Several research studies have shown that isolated anthraquinones from *Aloes* have antibacterial action [83]. They showed inhibition of *P. aeruginosa* [84]. While the mechanism of their antibacterial activity is still being investigated, it has been proposed that aloe-emodin and aloesin work by breaking bacterial membranes [83]. Aloe-emodin inhibited the biofilm formation and the extracellular protein synthesis of *S. aureus* [85]. Besides, phospholipids have a crucial role in biological membranes, providing structural, functional, and metabolic support [7]. Therefore, exogenous fatty acid exposure alters *P. aeruginosa* membrane phospholipid structure, membrane permeability as well as virulence [86].

LasR system is the main regulator of many genes including biofilm and virulence factors of *P. aeruginosa* QS. Its activation can positively impact gene expression. Blocking QS may reduce the pathogenicity of bacterial infections [87]. In the current study, docking results show the binding of the anthrones and anthraquinones identified from *A. marlothii* and *A. striata* extracts suggesting that their anti-virulence activity is a result of their interaction with LasR. In light of the above findings, it is necessary to validate the potential antimicrobial activities of these natural compounds, anthrones and anthraquinones, by conducting further in vivo studies to evaluate their safety profiles for use in clinical studies.

Conclusion

This study highlighted the mechanistic role of AMR and ASL as effective anti-virulence agents against *P. aeruginosa* via reducing biofilm development, decreasing pyocyanin production and limiting the swimming and swarming activity of *P. aeruginosa* for the first time. Furthermore, we applied HPLC–MS/MS to gain more insights into the differential chemical composition between the investigated species to detect the marker bioactive compounds, finding that the bioactive species, AMR and ASL, were rich with anthrones/anthraquinones. In this context, chrysophanol-8-*O*-glucoside and 6-malonylnataloin revealed higher binding affinities and stabilities within the binding pocket of LasR system, compared to TP-4, based on molecular docking. These findings support the use of AMR and ASL as natural alternatives for sustainable infections caused by *P. aeruginosa.*

Abbreviations

AML	*Aloe marlothii leaves*
AMR	*Aloe marlothii roots*
ASL	*Aloe striata leaves*
ASR	*Aloe striata roots*
PAO1	*Pseudomonas aeruginosa PAO1*

Acknowledgements

Not applicable.

Author contributions

P.M.A-B. contributed to conceptualization, methodology, investigation, funding acquisition, formal analysis, data curation, and writing—original draft. R.I. was involved in conceptualization, methodology, investigation, resources, and funding acquisition. N.E.M. contributed to conceptualization, methodology, investigation, resources, and funding acquisition. M.E.H. was involved in writing—original draft, review and editing, and data curation. M.A-E. contributed to visualization, resources, funding acquisition, and writing—review and editing. M. S.B. was involved in visualization, resources, funding acquisition, and writing—review and editing. M.H. contributed to visualization, writing—review and editing, formal analysis, and data curation. M.S. was involved in visualization, resources, and writing—review and editing.

Funding

Open access funding provided by The Science, Technology & Innovation Funding Authority (STDF) in cooperation with The Egyptian Knowledge Bank (EKB). This research received no external funding.

Availability of data and material

All data generated or analyzed during this study are included in this published article.

Declarations

Ethics approval and consent to participate

Not applicable.

Consent for publication

Not applicable.

Competing interests
The authors declare that they have no competing interests.

Author details
[1]Pharmacognosy Department, Faculty of Pharmacy, Cairo University, Kasr-El-Ainy Street, Cairo 11562, Egypt. [2]Department of Botany and Microbiology, Faculty of Science, Al-Azhar University, Cairo 11884, Egypt. [3]Department of Microbiology and Immunology, Faculty of Pharmacy (Girls), Al-Azhar University, Cairo, Egypt. [4]Pharmaceutical Chemistry Department, Faculty of Pharmacy, Cairo University, Kasr El-Aini Street, Cairo 11562, Egypt. [5]Agro-BioSciences Program, College of Agriculture and Environmental Sciences, University Mohammed VI Polytechnic, 43150 Ben Guerir, Morocco.

Received: 13 September 2024 Accepted: 29 June 2025
Published online: 18 July 2025

References

1. Arsene MMJ, Jorelle AB, Sarra S, Viktorovna PI, Davares AK, Ingrid NK, Steve AA, Vyacheslavovna YN, Carime BZ (2022) Short review on the potential alternatives to antibiotics in the era of antibiotic resistance. J Appl Pharm Sci 12:029–040. https://doi.org/10.7324/JAPS.2021.120102
2. WHO (2023) WHO fact sheet on antimicrobial resistance. https://www.who.int/news-room/fact-sheets/detail/antimicrobial-resistance (accessed 28 February 2023).
3. Tuon FF, Dantas LR, Suss PH, Tasca Ribeiro VS (2022) Pathogenesis of the *Pseudomonas aeruginosa* biofilm: a review. Pathogens 11:300. https://doi.org/10.3390/pathogens11030300
4. Qin S, Xiao W, Zhou C, Pu Q, Deng X, Lan L, Liang H, Song X, Wu M (2022) *Pseudomonas aeruginosa*: pathogenesis, virulence factors, antibiotic resistance, interaction with host, technology advances and emerging therapeutics. Signal Transduct Ther 7:199. https://doi.org/10.1038/s41392-022-01056-1
5. Thi MTT, Wibowo D, Rehm BH (2020) *Pseudomonas aeruginosa* biofilms. Int J Mol Sci 21:8671. https://doi.org/10.3390/ijms21228671
6. Hall S, McDermott C, Anoopkumar-Dukie S, McFarland AJ, Forbes A, Perkins AV, Davey AK, Chess-Williams R, Kiefel MJ, Arora D (2016) Cellular effects of pyocyanin, a secreted virulence factor of *Pseudomonas aeruginosa*. Toxins 8:236. https://doi.org/10.3390/toxins8080236
7. Okba MM, Baki PMA, Abu-Elghait M, Shehabeldine AM, El-Sherei MM, Khaleel AE, Salem MA (2022) UPLC-ESI-MS/MS profiling of the underground parts of common *Iris* species in relation to their anti-virulence activities against *Staphylococcus aureus*. J Ethnopharmacol 282:114658. https://doi.org/10.1016/j.jep.2021.114658
8. Baruah A, Bordoloi M, Baruah HPD (2016) *Aloe vera*: a multipurpose industrial crop. Ind Crops Prod 94:951–963. https://doi.org/10.1016/j.indcrop.2016.08.034
9. Anywar G, Tugume P, Kakudidi EK (2022) A review of aloe species used in traditional medicine in East Africa. S Afr J Bot 147:1027–1041. https://doi.org/10.1016/j.sajb.2021.07.036
10. Abera B (2014) Medicinal plants used in traditional medicine by Oromo people, Ghimbi District, Southwest Ethiopia. J Ethnobiol Ethnomed 10:1–15. https://doi.org/10.1186/1746-4269-10-40
11. Cock I (2015) The genus *Aloe*: Phytochemistry and therapeutic uses including treatments for gastrointestinal conditions and chronic inflammation. *In Novel natural products: therapeutic effects in pain, arthritis and gastro-intestinal diseases* 2015:179-235. Springer: Berlin, Germany, 2015, p.179-235
12. Kumar S, Yadav J (2014) Ethnobotanical and pharmacological properties of *Aloe vera*: a review. J Med Plants Res 48:1387–1398. https://doi.org/10.5897/JMPR2014.5336x
13. Bisrat D, Dagne E, van Wyk B-E, Viljoen A (2000) Chromones and anthrones from *Aloe marlothii* and *Aloe rupestris*. Phytochemistry 55:949–952. https://doi.org/10.1016/S0031-9422(00)00328-9
14. Wada G, Vincent M, Lee M (2018) Inner leaf gel of *Aloe striata* Induces adhesion-reducing morphological hyphal aberrations. J Fungi 4:23. https://doi.org/10.3390/jof4010023
15. Zapata P, Navarro D, Guillén F, Castillo S, Martínez-Romero D, Valero D, Serrano M (2013) Characterisation of gels from different *Aloe* spp. as antifungal treatment: Potential crops for industrial applications. Ind Crops Prod 42:223–230. https://doi.org/10.1016/j.indcrop.2012.06.002
16. Du Plessis LH, Hamman JH (2014) In vitro evaluation of the cytotoxic and apoptogenic properties of aloe whole leaf and gel materials. Drug Chem Toxicol 37:169–177. https://doi.org/10.3109/01480545.2013.834356
17. Fox LT, Du Plessis J, Gerber M, Van Zyl S, Boneschans B, Hamman JH (2014) In vivo skin hydration and anti-erythema effects of *Aloe vera*, *Aloe ferox* and *Aloe marlothii* gel materials after single and multiple applications. Pharmacogn Mag 10:S392. https://doi.org/10.4103/0973-1296.133291
18. Cardarelli M, Rouphael Y, Pellizzoni M, Colla G, Lucini L (2017) Profile of bioactive secondary metabolites and antioxidant capacity of leaf exudates from eighteen *Aloe* species. Ind Crops Prod 108:44–51. https://doi.org/10.1016/j.indcrop.2017.06.017
19. Andrea B, Dumitrița R, Florina C, Francisc D, Anastasia V, Socaci S, Adela P (2020) Comparative analysis of some bioactive compounds in leaves of different *Aloe* species. BMC Chem 14:1–11. https://doi.org/10.1186/s13065-020-00720-3
20. Mianda SM, Invernizzi L, van der Watt ME, Reader J, Moyo P, Birkholtz L-M, Maharaj VJ (2022) *In vitro* dual activity of *Aloe marlothii* roots and its chemical constituents against *Plasmodium falciparum* asexual and sexual stage parasites. J Ethnopharmacol 297:115551. https://doi.org/10.1016/j.jep.2022.115551
21. Ibrahim RM, Mahdy NE, Abdel-Baki PM, El Badawy SA, Ali SE, Ibrahim MA, Khattab MS, Farroh KY, Emam SR (2023) Chemical characterization, in vitro and in vivo evaluation of chitosan-*Aloe marlothii* gel loaded nanoparticles on acetaminophen-induced hepatitis in mice. S Afr J Bot 157:1–9. https://doi.org/10.1016/j.sajb.2023.03.044
22. Mahdy NE, Ibrahim RM, Abdel-Baki PM, Emam SR, Ali SE, Ibrahim MA, Khattab MS, Farroh KY, Badawy SAE (2024) Hepatoprotective mechanisms of chemically characterized *Aloe striata* gel with and without loading on nanoparticles, involving ERK-JNK signaling pathway. S Afr J Bot 170:163–171. https://doi.org/10.1016/j.sajb.2024.05.024
23. Soliman MK, Salem SS, Abu-Elghait M, Azab MS (2023) Biosynthesis of silver and gold nanoparticles and their efficacy towards antibacterial, antibiofilm, cytotoxicity, and antioxidant activities. Appl Biochem Biotechnol 195:1158–1183. https://doi.org/10.1007/s12010-022-04199-7
24. Soliman MK, Abu-Elghait M, Salem SS, Azab MS (2022) Multifunctional properties of silver and gold nanoparticles synthesis by Fusarium pseudonygamai. Biomass Convers Biorefin. https://doi.org/10.1007/s13399-022-03507-9
25. Khattab AM, Abo-Taleb HA, Abdelaziz AM, El-Tabakh MA, El-Feky MM, Abu-Elghait M (2022) Daphnia magna and Gammarus pulex, novel promising agents for biomedical and agricultural applications. Sci Rep 12:13690. https://doi.org/10.1038/s41598-022-17790-z
26. Yousef A, Abu-Elghait M, Barghoth MG, Elazzazy AM, Desouky SE (2022) Fighting multidrug-resistant *Enterococcus faecalis* via interfering with virulence factors using green synthesized nanoparticles. Microb Pathog 173:105842. https://doi.org/10.1016/j.micpath.2022.105842
27. Wang J, Liu H, Zhao J, Gao H, Zhou L, Liu Z, Chen Y, Sui P (2010) Antimicrobial and antioxidant activities of the root bark essential oil of *Periploca sepium* and its main component 2-hydroxy-4-methoxybenzaldehyde. Molecules 15:5807–5817. https://doi.org/10.3390/molecules15085807
28. Essar DW, Eberly L, Hadero A, Crawford I (1990) Identification and characterization of genes for a second anthranilate synthase in *Pseudomonas aeruginosa*: interchangeability of the two anthranilate synthases and evolutionary implications. J Bacteriol 172:884–900. https://doi.org/10.1128/jb.172.2.884-900.1990
29. Nassar O, Desouky SE, El-Sherbiny GM, Abu-Elghait M (2022) Correlation between phenotypic virulence traits and antibiotic resistance in *Pseudomonas aeruginosa* clinical isolates. Microb Pathog 162:105339. https://doi.org/10.1016/j.micpath.2021.105339
30. Murray TS, Ledizet M, Kazmierczak BI (2010) Swarming motility, secretion of type 3 effectors and biofilm formation phenotypes exhibited within a large cohort of *Pseudomonas aeruginosa* clinical isolates. J Med Microbiol 59:511. https://doi.org/10.1099/jmm.0.017715-0
31. Raoof W, Latif I (2010) In vitro study of the swarming phenomena and antimicrobial activity of pyocyanin produced by *Pseudomonas aeruginosa* isolated from different human infections. Eur J Sci Res 47:405
32. Tawfeek N, Fikry E, Mahdi I, Ochieng MA, Bakrim WB, Taarji N, Mahmoud MF, Sobeh M (2023) *Cupressus arizonica* greene: phytochemical profile

and cosmeceutical and dermatological properties of its leaf extracts. Molecules 28:1036. https://doi.org/10.3390/molecules28031036
33. Quispe C, Villalobos M, Bórquez J, Simirgiotis M (2018) Chemical composition and antioxidant activity of *Aloe vera* from the Pica Oasis (Tarapacá, Chile) by UHPLC-Q/Orbitrap/MS/MS. J Chem 2018:1–12. https://doi.org/10.1155/2018/6123850
34. Añibarro-Ortega M, Pinela J, Barros L, Ćirić A, Silva SP, Coelho E, Mocan A, Calhelha RC, Soković M, Coimbra MA (2019) Compositional features and bioactive properties of *Aloe vera* leaf (fillet, mucilage, and rind) and flower. Antioxidants 8:444. https://doi.org/10.3390/antiox8100444
35. Breaud C, Lallemand L, Mares G, Mabrouki F, Bertolotti M, Simmler C, Greff S, Mauduit M, Herbette G, Garayev E (2023) LC-MS Based phytochemical profiling towards the identification of antioxidant markers in some endemic *Aloe* species from Mascarene Islands. Antioxidants 12:50. https://doi.org/10.3390/antiox12010050
36. El Sayed AM, Ezzat SM, El Naggar MM, El Hawary SS (2016) *In vivo* diabetic wound healing effect and HPLC-DAD-ESI-MS/MS profiling of the methanol extracts of eight *Aloe* species. Rev Bras Farmacogn 26:352–362. https://doi.org/10.1016/j.bjp.2016.01.009
37. Wu X, Ding W, Zhong J, Wan J, Xie Z (2013) Simultaneous qualitative and quantitative determination of phenolic compounds in *Aloe barbadensis* Mill by liquid chromatography–mass spectrometry-ion trap-time-of-flight and high performance liquid chromatography-diode array detector. J Pharm Biomed Anal 80:94–106. https://doi.org/10.1016/j.jpba.2013.02.034
38. Fan J, Li C, Hu Y, Chen H, Yang F (2018) Comparative assessment of in vitro thrombolytic and fibrinolysis activity of four *Aloe* species and analysis of their phenolic compounds by LC–MS. S Afr J Bot 119:325–334. https://doi.org/10.1016/j.sajb.2018.10.001
39. Zhong J-S, Wan J-Z, Ding W-J, Wu X-F, Xie Z-Y (2015) Multi-responses extraction optimization combined with high-performance liquid chromatography-diode array detection–electrospray ionization-tandem mass spectrometry and chemometrics techniques for the fingerprint analysis of *Aloe barbadensis* Miller. J Pharm Biomed Anal 107:131–140. https://doi.org/10.1016/j.jpba.2014.12.032
40. Otify AM, Ibrahim RM, Abib B, Laub A, Wessjohann LA, Jiang Y, Farag MA (2023) Unveiling metabolome heterogeneity and new chemicals in 7 tomato varieties via multiplex approach of UHPLC-MS/MS, GC–MS, and UV–Vis in relation to antioxidant effects as analyzed using molecular networking and chemometrics. Food Chem 417:135866. https://doi.org/10.1016/j.foodchem.2023.135866
41. Ramabulana A-T, Steenkamp P, Madala N, Dubery IA (2020) Profiling of chlorogenic acids from Bidens pilosa and differentiation of closely related positional isomers with the aid of UHPLC-QTOF-MS/MS-based in-source collision-induced dissociation. Metabolites 10:178. https://doi.org/10.3390/metabo10050178
42. Willems JL, Khamis MM, Saeid WM, Purves RW, Katselis G, Low NH, El-Aneed A (2016) Analysis of a series of chlorogenic acid isomers using differential ion mobility and tandem mass spectrometry. Anal Chim Acta 933:164–174. https://doi.org/10.1016/j.aca.2016.05.041
43. Ncube EN, Mhlongo MI, Piater LA, Steenkamp PA, Dubery IA, Madala NE (2014) Analyses of chlorogenic acids and related cinnamic acid derivatives from *Nicotiana tabacum* tissues with the aid of UPLC-QTOF-MS/MS based on the in-source collision-induced dissociation method. Chem Cent J 8:1–10. https://doi.org/10.1186/s13065-014-0066-z
44. Clifford MN, Johnston KL, Knight S, Kuhnert N (2003) Hierarchical scheme for LC-MS n identification of chlorogenic acids. J Agric Food Chem 51:2900–2911. https://doi.org/10.1021/jf026187q
45. Attia YM, El-Kersh DM, Wagdy HA, Elmazar MM (2018) Verbascoside: Identification, quantification, and potential sensitization of colorectal cancer cells to 5-FU by targeting PI3K/AKT pathway. Sci Rep 8:16939. https://doi.org/10.1038/s41598-018-35083-2
46. Hamed AR, El-Hawary SS, Ibrahim RM, Abdelmohsen UR, El-Halawany AM (2021) Identification of chemopreventive components from halophytes belonging to Aizoaceae and Cactaceae through LC/MS—Bioassay guided approach. J Chromatogr Sci 59:618–626. https://doi.org/10.1093/chromsci/bmaa112
47. Aabideen ZU, Mumtaz MW, Akhtar MT, Raza MA, Mukhtar H, Irfan A, Raza SA, Touqeer T, Nadeem M, Saari N (2021) *Cassia fistula* Leaves; UHPLC-QTOF-MS/MS based metabolite profiling and molecular docking insights to explore bioactives role towards inhibition of pancreatic lipase. Plants 10:1334. https://doi.org/10.3390/plants10071334
48. Aldayel TS, Grace MH, Lila MA, Yahya MA, Omar UM, Alshammary G (2020) LC-MS characterization of bioactive metabolites from two Yemeni Aloe spp. with antioxidant and antidiabetic properties. Arab J Chem 13:5040–5049. https://doi.org/10.1016/j.arabjc.2020.02.003
49. Luo D, He M, Li J, Du H, Mao Q, Pei N, Zhong G, Ouyang H, Yang S, Feng Y (2021) Integrating the rapid constituent profiling strategy and multivariate statistical analysis for herb ingredients research, with Chinese official rhubarb and Tibetan rhubarb as an example. Arab J Chem 14:103269. https://doi.org/10.1016/j.arabjc.2021.103269
50. Li T, Liao Z, Chen M, Liu D, Zhang S, Lin L, Zheng H, Liao Q, Xie Z, Song F (2018) Simultaneous qualitative and quantitative determination of compounds in Aloe arborescens Mill using liquid chromatography with ion trap time-of-flight mass spectrometry and diode array detectors. Sep Sci Plus 1:640–649. https://doi.org/10.1002/sscp.201700048
51. Viljoen AM, Van Wyk B-E (2000) The chemotaxonomic significance of the phenyl pyrone aloenin in the genus *Aloe*. Biochem Syst Ecol 28:1009–1017. https://doi.org/10.1016/S0305-1978(00)00018-1
52. Ferreres F, Silva BM, Andrade PB, Seabra RM, Ferreira MA (2003) Approach to the study of C-glycosyl flavones by ion trap HPLC-PAD-ESI/MS/MS: application to seeds of quince (*Cydonia oblonga*). Phytochem Anal 14:352–359. https://doi.org/10.1002/pca.727
53. Elmi A, Mohamed Abdoul-Latif F, Spina R, Dupire F, Philippot S, Marie-France C, Jacobs H, Laurain-Mattar D (2021) *Aloe djiboutiensis*: antioxidant activity, molecular networking-based approach and in vivo toxicity of this endemic species in Djibouti. Molecules 26:3046. https://doi.org/10.3390/molecules26103046
54. Dagne E, Bisrat D, Viljoen A, Van Wyk B-E (2000) Chemistry of *Aloe* species. Curr Org Chem 4:1055–1078. https://doi.org/10.2174/1385272003375932
55. Silva ACR, Garrett R, Rezende CM, Meckelmann SW (2022) Lipid characterization of arabica and robusta coffee beans by liquid chromatography-ion mobility-mass spectrometry. J Food Compost Anal 111:104587. https://doi.org/10.1016/j.jfca.2022.104587
56. Huang W, Lan L, Zhou H, Yuan J, Mao X, Hu Q, Ji S (2022) Comprehensive profiling of *Platycodonis radix* in different growing regions using liquid chromatography coupled with mass spectrometry: from metabolome and lipidome aspects. RSC Adv 12:3897–3908. https://doi.org/10.1039/D1RA08285J
57. Zhu J, Zhou L, Zhao M, Wei F, Fu H, Marchioni E (2023) Revealing the dynamic changes of lipids in coffee beans during roasting based on UHPLC-QE-HR-AM/MS/MS. Food Res Int 174:113507. https://doi.org/10.1016/j.foodres.2023.113507
58. York T, Van Vuuren S, De Wet H (2012) An antimicrobial evaluation of plants used for the treatment of respiratory infections in rural Maputaland, KwaZulu-Natal, South Africa. J Ethnopharmacol 144:118–127. https://doi.org/10.1016/j.jep.2012.08.038
59. Luseba D, Elgorashi E, Ntloedibe D, Van Staden J (2007) Antibacterial, anti-inflammatory and mutagenic effects of some medicinal plants used in South Africa for the treatment of wounds and retained placenta in livestock. S Afr J Bot 73:378–383. https://doi.org/10.1016/j.sajb.2007.03.003
60. Bisi-Johnson MA, Obi CL, Hattori T, Oshima Y, Li S, Kambizi L, Eloff JN, Vasaikar SD (2011) Evaluation of the antibacterial and anticancer activities of some South African medicinal plants. BMC Complement Altern Med 11:1–5. https://doi.org/10.1186/1472-6882-11-14
61. Bisi-Johnson MA, Obi CL, Samuel BB, Eloff JN, Okoh AI (2017) Antibacterial activity of crude extracts of some South African medicinal plants against multidrug resistant etiological agents of diarrhoea. BMC Complement Altern Med 17:1–9. https://doi.org/10.1186/s12906-017-1802-4
62. Khunoana ET, Madikizela B, Erhabor JO, Nkadimeng SM, Arnot L, Van Wyk I, McGaw LJ (2019) A survey of plants used to treat livestock diseases in the Mnisi community, Mpumalanga, South Africa, and investigation of their antimicrobial activity. S Afr J Bot 126:21–29. https://doi.org/10.1016/j.sajb.2019.07.026
63. Shirinda H, Leonard C, Candy G, Van Vuuren S (2019) Antimicrobial activity and toxicity profile of selected southern African medicinal plants against neglected gut pathogens. S Afr J Sci 115:1–10
64. Yeo SS-M, Tham F-Y (2012) Anti-quorum sensing and antimicrobial activities of some traditional Chinese medicinal plants commonly used in South-East Asia. Malays J Microbiol 8:11–20

65. Doğanlı GA (2016) Phenolic content and antibiofilm activity of propolis against clinical MSSA strains. Records of Natural Products
66. Othman L, Sleiman A, Abdel-Massih RM (2019) Antimicrobial activity of polyphenols and alkaloids in middle eastern plants. Front Microbiol 10:911. https://doi.org/10.3389/fmicb.2019.00911
67. Lawrence R, Tripathi P, Jeyakumar E (2009) Isolation, purification and evaluation of antibacterial agents from *Aloe vera*. Braz J Microbiol 40:906–915. https://doi.org/10.1590/S1517-83822009000400023
68. Kouassi Y, Shelef LA (1998) Inhibition of *Listeria monocytogenes* by cinnamic acid: possible interaction of the acid with cysteinyl residues. J Food Saf 18:231–242. https://doi.org/10.1111/j.1745-4565.1998.tb00217.x
69. Weir TL, Park S-W, Vivanco JM (2004) Biochemical and physiological mechanisms mediated by allelochemicals. Curr Opin Plant Biol 7:472–479. https://doi.org/10.1016/j.pbi.2004.05.007
70. Silva S, Costa EM, Horta B, Calhau C, Morais RM, Pintado MM (2016) Antibiofilm potential of phenolic acids: the influence of environmental pH and intrinsic physico-chemical properties. Biofouling 32:853–860. https://doi.org/10.1080/08927014.2016.1208183
71. Ugurlu A, Yagci AK, Ulusoy S, Aksu B, Bosgelmez-Tinaz G (2016) Phenolic compounds affect production of pyocyanin, swarming motility and biofilm formation of *Pseudomonas aeruginosa*. Asian Pac JTrop Biomed 6:698–701. https://doi.org/10.1016/j.apjtb.2016.06.008
72. Coppo E, Marchese A (2014) Antibacterial activity of polyphenols. Curr Pharm Biotechnol 15:380–390. https://doi.org/10.2174/1389201015 04140825121142
73. Koz O, Pizza C, Kırmızıgül S (2009) Triterpene and flavone glycosides from Anchusa undulata subsp. hybrida. Nat Prod Res 23:284–292. https://doi.org/10.1080/14786410802006140
74. Megeressa M, Bisrat D, Mazumder A, Asres K (2015) Structural elucidation of some antimicrobial constituents from the leaf latex of *Aloe trigonantha* LC Leach. BMC Complement Altern Med 15:1–7. https://doi.org/10.1186/s12906-015-0803-4
75. Hiruy M, Bisrat D, Mazumder A, Asres K (2021) Two chromones with antimicrobial activity from the leaf latex of *Aloe monticola* Reynolds. Nat Prod Res 35:1052–1056. https://doi.org/10.1080/14786419.2019.1614581
76. Añibarro-Ortega M, Pinela J, Ćirić A, Lopes E, Molina AK, Calhelha RC, Soković M, Ferreira O, Ferreira IC, Barros L (2021) Extraction of aloesin from *Aloe vera* rind using alternative green solvents: process optimization and biological activity assessment. Biology 10:951. https://doi.org/10.3390/biology10100951
77. Trognon J, Vera G, Rima M, Stigliani J-L, Amielet L, El Hage S, Lajoie B, Roques C, El Garah F (2022) Investigation of direct and retro chromone-2-carboxamides based analogs of *Pseudomonas aeruginosa* quorum sensing signal as new anti-biofilm agents. Pharmaceuticals 15:417. https://doi.org/10.3390/ph15040417
78. Biharee A, Sharma A, Kumar A, Jaitak V (2020) Antimicrobial flavonoids as a potential substitute for overcoming antimicrobial resistance. Fitoterapia 146:104720. https://doi.org/10.1016/j.fitote.2020.104720
79. Geethalakshmi R, Sundaramurthi JC, Sarada DV (2018) Antibacterial activity of flavonoid isolated from *Trianthema decandra* against *Pseudomonas aeruginosa* and molecular docking study of FabZ. Microb Pathog 121:87–92. https://doi.org/10.1016/j.micpath.2018.05.016
80. Induli M, Cheloti M, Wasuna A, Wekesa I, Wanjohi JM, Byamukama R, Heydenrich M, Makayoto M, Yenesew A (2012) Naphthoquinones from the roots of *Aloe secundiflora*. Phytochem Lett 5:506–509
81. Wu YW, Ouyang J, Xiao XH, Gao WY, Liu Y (2006) Antimicrobial properties and toxicity of anthraquinones by microcalorimetric bioassay. Chin J Chem 24:45–50. https://doi.org/10.1002/cjoc.200690020
82. Xiang W, Song Q-S, Zhang H-J, Guo S-P (2008) Antimicrobial anthraquinones from *Morinda angustifolia*. Fitoterapia 79:501–504. https://doi.org/10.1016/j.fitote.2008.04.008
83. Alves DS, Pérez-Fons L, Estepa A, Micol V (2004) Membrane-related effects underlying the biological activity of the anthraquinones emodin and barbaloin. Biochem Pharmacol 68:549–561. https://doi.org/10.1016/j.bcp.2004.04.012
84. Qun T, Zhou T, Hao J, Wang C, Zhang K, Xu J, Wang X, Zhou W (2023) Antibacterial activities of anthraquinones: structure–activity relationships and action mechanisms. RSC Med Chem 14:1446–1471. https://doi.org/10.1039/D3MD00116D
85. Xiang H, Cao F, Ming D, Zheng Y, Dong X, Zhong X, Mu D, Li B, Zhong L, Cao J (2017) Aloe-emodin inhibits *Staphylococcus aureus* biofilms and extracellular protein production at the initial adhesion stage of biofilm development. Appl Microbiol Biotechnol 101:6671–6681. https://doi.org/10.1007/s00253-017-8403-5
86. Baker LY, Hobby CR, Siv AW, Bible WC, Glennon MS, Anderson DM, Symes SJ, Giles DK (2018) *Pseudomonas aeruginosa* responds to exogenous polyunsaturated fatty acids (PUFAs) by modifying phospholipid composition, membrane permeability, and phenotypes associated with virulence. BMC Microbiol 18:1–12. https://doi.org/10.1186/s12866-018-1259-8
87. Mizdal CR, Stefanello ST, Nogara PA, Soares FAA, de Lourenço ML, de Campos MMA (2018) Molecular docking, and anti-biofilm activity of gold-complexed sulfonamides on *Pseudomonas aeruginosa*. Microb Pathog 125:393–400. https://doi.org/10.1016/j.micpath.2018.10.004
88. Abdel-Baki PM, Mahdy NE, Ibrahim RM, El Badawy SA, Ali SE, Ibrahim MA, Khattab MS, El-Rashedy AA, Emam SR (2025) Phytochemical analysis and neuroprotective potential of *Achillea santolina L.* fractions. Sci Rep 15(1):16070. https://doi.org/10.1038/s41598-025-98887-z

Publisher's Note

Springer Nature remains neutral with regard to jurisdictional claims in published maps and institutional affiliations.